IEICE TRANS. ELECTRON., VOL.E100–C, NO.3 MARCH 2017

INVITED PAPER *Special Section on Leading-Edge Technologies of Superconducting Measurement Systems*

Recent Progress and Application of Superconducting Nanowire Single-Photon Detectors

Taro YAMASHITA[†a)], **Shigehito MIKI**[†], ***and*** **Hirotaka TERAI**[†], ***Members***

SUMMARY In this review, we present recent advances relating to superconducting nanowire single-photon detectors (SSPDs or SNSPDs) and their broad range of applications. During a period exceeding ten years, the system performance of SSPDs has been drastically improved, and lately excellent detection efficiencies have been realized in practical systems for a wide range of target photon wavelengths. Owing to their advantages such as high system detection efficiency, low dark count rate, and excellent timing jitter, SSPDs have found application in various research fields such as quantum information, quantum optics, optical communication, and also in the life sciences. We summarize the photon detection principle and the current performance status of practical SSPD systems. In addition, we introduce application examples in which SSPDs have been applied.

key words: *superconductivity, single-photon detector, quantum information, quantum optics, optical communication, life science*

1. Introduction

Since the first demonstration of a superconducting nanowire single-photon detector (SSPD or SNSPD) by Goltsman *et al*. in 2001 [1], its performance has been improved drastically and, consequently, SSPD systems have already been put into practical use [2]. Currently, several companies actually produce practical SSPD systems on a commercial basis. The most remarkable progress in the development of SSPDs is the significant improvement of the system detection efficiency (SDE) for telecommunication-wavelength photons. The SDE is the pulse output probability for incident photons into the system, and consists of four factors: the optical coupling efficiency between the device and the incident photon flux, the optical absorptance in the superconducting nanowire, the intrinsic efficiency after photon absorption, and the total optical loss of the system [3].

In 2013, as a result of an effort to improve all of these factors, a world record was set by achieving an SDE of 93% for a tungsten silicide (WSi) nanowire by a group from NIST [4], and excellent SDEs around 80% have been reported with niobium nitride (NbN) [5] and niobium titanium nitride (NbTiN) [6] by MIT and NICT groups, respectively. The achievement of high-SDE single-photon detectors has a broad impact on various research fields using telecommunication-wavelength photons such as quantum information, quantum optics, and optical communication because the conventionally used indium gallium arsenide (InGaAs) avalanche photodiode (APD) has an SDE as low as ∼10% [7].

Recently, SSPDs have also been developed for shorter wavelength photons including those in the visible region. Optimization of the optical cavity structure has enabled the SDE for visible wavelengths to be improved to ∼80% comparable to that for telecommunication wavelengths [8]. Although the conventional silicon APD (Si APD) also has good efficiency of ∼60–70% for a wavelength of 650 nm, it exhibits afterpulsing noise after a photon detection event, and therefore afterpulsing-free characteristics of SSPDs is a clear advantage for certain kinds of correlation experiments such as fluorescence correlation spectroscopy in the life science field [9], [10].

In this review, we present recent progress of SSPDs and their application to a variety of research fields. In the next section, we briefly introduce the photon detection mechanisms of SSPD. Then, in Sect. 3, we summarize the latest performance of SSPDs from visible to telecommunication wavelengths. In Sects. 4–7, we introduce SSPD applications to quantum information, optical space telecommunication, life science, quantum optics, and others.

2. Photon-Detection Principle of SSPD

In an SSPD, the active area receiving photons consists of meandering superconducting nanowire with a thickness of a few nanometers. A bias current less than the switching current is constantly applied to the nanowire during the operation of the detector [1]. The basic process of photon detection by an SSPD is as follows: (i) Single photon is absorbed in the superconducting nanowire. (ii) In the absorbed region, superconductivity is locally weakened due to energy excitation by the single photon. (iii) The bias current brings the weakened region to the resistive state and the resistive region finally crosses the nanowire. (iv) The bias current escapes to the load side, causing a voltage pulse. (v) The resistive region recovers to the superconducting state through a thermal relaxation process.

The microscopic physical mechanism in the nanowire after absorbing an incident photon is still under discussion. In the early stages, a “hotspot” model was presented to understand the resistive-state transition by photon absorption [1], [11]. In this model, when the photon enters the nanowire, the normal-state core (hotspot) is generated by the energy excitation of the quasiparticles. Then the bias current escapes to around the resistive hotspot in the nanowire.

Manuscript received August 8, 2016.
Manuscript revised November 20, 2016.
[†]The authors are with NICT Advanced ICT Research Institute, Kobe-shi, 651–2492 Japan.
a) E-mail: taro@nict.go.jp
DOI: 10.1587/transele.E100.C.274

Table 1 Summary of SSPD performance for various wavelengths of a single photon.

Target wavelength (nm)	Material	SDE	CR@3dB loss (MHz)	Jitter (ps)	Operation temp. (K)	Active area	Coupling	Fiber	Reference and note
1550	WSi	93	-	150	0.12 (ADR)	$15 \times 15\ \mu m^2$	Self-alignment	SM	[4]
	MoSi	82	4	99	2.3	$16 \times 16\ \mu m^2$	Self-alignment	SM	[23]
		87	-	76	0.7 (^{4}He)				
	NbN	76	300	60-80	2.5	14 μm diameter	Nano-positioner	SM	[5], 4 element array
	NbN	80	6-16	-	2.1	$15 \times 15\ \mu m^2$	Fiber-coupled package	SM with lens	[22], Low filling factor for 16-MHz CR
	NbTiN	77	-	68	2.3	$15 \times 15\ \mu m^2$	Fiber-coupled package	SM with lens	[6]
		83	-	-	0.3 (^{3}He)				
1310	WSi	78	-	191	2.5	$16 \times 16\ \mu m^2$	Self-alignment	SM	[24]
940	NbN	84	-	63	2.3	$18 \times 18\ \mu m^2$	Fiber-coupled package	SM	[33]
850	NbN	82	-	105	2.1	50 μm diameter	Fiber-coupled package	MM with lens	[34]
670-850	NbN	74-86	-	-	2.2	$15 \times 15\ \mu m^2$	Fiber-coupled package	SM	[32]
635	NbN	73	8.5	76	2.2	35 μm diameter	Fiber-coupled package	MM with lens	[8]
520-530	NbN	64	-	-	2.2	35 μm diameter	Fiber-coupled package	MM with lens	[32], 4 element array
		75	-	140	2.1	42 μm diameter	Fiber-coupled package	MM with lens	[35]

When the current density exceeds the critical current density of the nanowire, the normal-state region expands across the nanowire, and finally a finite resistance appears.

As another possible mechanism, vortex-induced photon detection has been proposed [12]. In this model, the incident photon creates a weak superconducting (not the normal state) region by the excitation of quasiparticles, and then the vortex or vortex-antivortex pair is generated in the nanowire. The vortices move to the edge of the nanowire due to the Lorentz force by the bias current. As a result, a finite resistance appears because a normal belt is generated due to dissipation by the vortex crossing across the nanowire. *Note that this photon detection concept was already presented by Kadin over ten years ago for the first SSPD demonstration* [13]. In recent years, a number of studies have been performed to clarify the detection mechanism of an SSPD by using various approaches such as detector tomography [14], [15], magnetic response [16], and numerical simulation [17], [18], but further studies, both experimental and theoretical, are required to confirm the detection mechanism. On the other hand, regarding the dark count, which is the error output count without incident photons, a current-induced vortex crossing has been proposed as a plausible origin [19]–[21].

3. SSPD Performance in Practical Systems

In this section, we present a summary of current SSPD performance with a focus on SDE for various photon wavelengths. To date, the main target of SSPD has been telecommunication wavelengths ranging from 1300 to 1600 nm. As shown in Table 1, excellent SDEs of 80–90% for 1550-nm-wavelength photons have been reported by using various superconducting materials in SSPDs [4]–[6], [22]–[24]. The NIST group demonstrated the highest SDE of 93% for amorphous WSi nanowire at an operation temperature of 120 mK [4]. A well-saturated SDE in the bias dependence, which is favorable to stable performance, has been obtained although a relatively large adiabatic demagnetization (ADR) cryocooler was required to cool down the WSi nanowire to a low superconducting critical temperature of 3.7 K. MIT [5] and NICT [6] have presented high SDEs of around 80% at 2 K for NbN or NbTiN SSPDs mounted in the compact Gifford-McMahon (GM) cryocooler, which is suitable for wide-range applications. Recently, new candidates for the nanowire material of SSPD, such as MoSi [23] and MoGe [25] have also been studied, and an excellent SDE of 82% at 2.3 K was reported for the MoSi SSPD. The most effective superconducting material for the nanowire of an SSPD is still being explored experimentally, and in future theoretical suggestions are highly demanded in parallel with the clarification of the detection physics. From an engineering viewpoint, a common key point to realize these high SDEs is the optical cavity structure to enhance the photon absorptance [3]. By placing the nanowire between upper and lower dielectric layers consisting of materials such as SiO and SiO_2, incident photons are strongly confined around the nanowire and thus almost perfect absorptance can be realized, leading to a high SDE. Another key technique is an efficient optical coupling method between the incident photons from the single-mode (SM) optical fiber and the SSPD active area. Mainly three coupling methods have been presented: self-alignment [26], a fiber-coupled package [6], [27], and nanopositioner alignment [5], all of which are able to realize highly efficient coupling. For more detail of the device design and mount, readers are referred to a recent review [2].

Several challenges to reduce the dark count rate (DCR) also have been presented [28], [29]. The DCR of SSPDs consists of intrinsic one due to the energy dissipation in the nanowire [19]–[21] and extrinsic one originated from the blackbody radiation at room temperature through the opti-

cal fiber [30]. Regarding the reduction of the extrinsic DCR, Shibata *et al*. realized SSPDs with ultralow DCR by adopting cold optical band-pass filters [28]. It has been shown that the extrinsic DCR could be reduced by using cold optical bending fiber [29]. Furthermore, SSPDs with a dielectric multilayer designed to cut the extrinsic DCR also have been presented [31], [32].

Another great advantage of the SSPD is the broadband sensitivity of the superconducting nanowire. Especially, shorter wavelength photons can be detected easier than telecom photons because the higher energy photons can destroy the superconducting state of the nanowire more effectively. Recently, excellent SDEs of around 80% have been reported for various wavelengths ranging from visible (~500 nm) to near infrared (~1000 nm) [8], [32]–[35]. Maximization of the optical absorbance at the desired wavelength was achieved by optically designing a dielectric mirror consisting of multilayers of two kinds of dielectric materials, such as SiO_2 and TiO_2, on the substrate. More recently, a non-periodic dielectric multilayer structure enabling the flexible spectrum (wavelength dependence) design of the optical absorbance in the SSPD was presented [32]. In short-wavelength applications, such as those in the life sciences, a multimode (MM) fiber with a large core is often used to introduce free-space light efficiently. Thus, in order to realize high optical coupling efficiency to the incident light from the MM fiber, large-active-area SSPDs with a diameter over 30 μm have often been prepared.

The maximum counting rate (CR) is also an important performance factor of a single-photon detector. Although the intrinsic recovery time from the resistive state to the superconducting state in the nanowire is expected to be very short (as short as several tens of picoseconds), the maximum CR of the SSPD is limited by the kinetic inductance of the nanowire and the actual CR at the 3-dB cutoff of SDE is approximately 10 MHz [36]. For the same material, a longer, narrower, thinner nanowire leads to a longer reset time, i.e., a lower maximum CR [22]. This indicates that there is a trade-off between the SDE and CR because the small active area produced by using a short nanowire to obtain high CR has poor optical coupling efficiency. An effective solution to this problem is to make a multi-element array structure because the nanowire length of each element can be reduced with keeping the total active area enough to couple with the incident light [5]. To the present, an SSPDs with 64 elements have been fabricated and demonstrated as the maximum number of elements [37], [38]. Further work is in progress to enlarge the size of the active area. In addition, the signal processing of the output from the each element is also crucial for the multi-element SSPD array system, and several cryogenic processing techniques such as single-flux-quantum (SFQ) and SiGe IC are being developed [39], [40].

As described above, the performance of SSPD systems has been considerably improved during a period of more than ten years. Here it should be noted that there are already several private companies selling commercial SSPD systems around the world, e.g., *Scontel* (Russia), *Photon Spot* (USA), *Single Quantum* (The Netherlands), *Quantum Opus* (USA), and *ID Quantique* (Switzerland). Thus, for researchers working in the various fields requiring a highly precise single-photon detection technique, it becomes easier to use a high-performance practical SSPD system.

4. Quantum Communication

One of striking applications of SSPDs is quantum key distribution (QKD) which guarantees unconditional security based on the laws of physics and is a core technology for the realization of a quantum communication network [41]. In 2007, Takesue *et al*. were the first to demonstrate quantum distribution over a 200-km optical fiber with a 42-dB loss by using SSPDs [42]. Although the detection efficiency at that time was very small (0.7%), the low DCR of a few Hz and small 60-ps timing jitter of the SSPDs led to the successful achievement of a long distance QKD experiment.

In 2010, field test of QKD in a metropolitan area of Japan. This network, named the Tokyo QKD network, was implemented by an international team consisting of nine organizations (Fig. 1 (a)) [43]. The demonstration entailed the presentation of a secure TV conference between two points separated by a distance of more than 45 km by using secure keys carried thorough the open testbed fiber network. SSPDs with an SDE of over 10% were installed in the Tokyo QKD network. Recently, differential phase shift QKD over 336 km with 72 dB channel loss using the SSPD with the ultralow DCR of 0.01 cps have been reported [44]. The advantages of SSPDs in the form of afterpulse-free properties, the absence of gate timing control, and low DCR contributed to an improvement of the QKD system.

In order to realize quantum communication system, a long-distance entanglement distribution is also important, and recently experiments of an entanglement distribution over 300 km of the optical fiber has been achieved by using SSPDs [45]. Very recently, a new scheme named the measurement-device-independent QKD (MDI-QKD) protocol, in which the security never relies on the measurement, has been actively studied, and high-performance SSPDs were implemented also in the MDI-QKD systems as a key device [46].

5. Optical Space Telecommunication

In recent years, SSPD has been playing an essential role in the realization of optical telecommunication in the cosmic space [47]. In 2013, NASA successfully achieved the Lunar Laser Communication Demonstration (LLCD). The LLCD project tested a free-space communication network based on optical technology, which realizes a higher data rate, compact setup, and less power consumption compared to the conventional radio frequency (RF) technique (Fig. 1 (b)). The earth-based terminal forming part of this project, the Lunar Lasercom Ground Terminal (LLGT), for which a photon-counting receiver consisting of an NbN SSPD array with an SDE of ~75% was installed, was developed

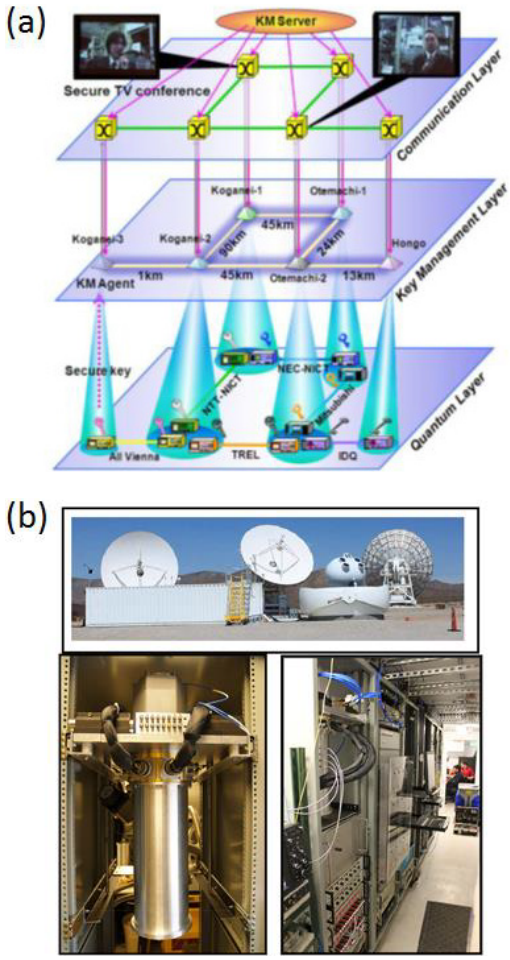

Fig. 1 (a) Three-layer architecture of the Tokyo QKD Network [43]. It consists of a quantum, key management, and communication layer. (b) Top: The Lunar Lasercom Ground Terminal (LLGT) at White Sands, New Mexico [47]. Bottom right: The rack-mounted cryogenic refrigerator for the four 4-element SNSPD arrays with four multimode weakly polarization-maintaining fiber inputs in the LLGT control room. Bottom left: Cryogenic refrigerator rack alongside additional electronic signal processing racks in the LLGT control room.

for this project. In addition, the maximum counting rate of the SSPD was improved by adopting an interleaved four-element array structure in a 14-μm-diameter circular active area. Finally, the LLCD demonstrated communication with the longest range and highest rate between the earth and the moon by achieving a data rate of 622 Mb/s for the error-free down link from the space optical terminal on the lunar-orbiting satellite to the LLGT [47].

More recently, toward the realization of the deep-space optical communication (DSOC) system connection between the earth and the mars, JPL is working on a WSi SSPD array with a large active area for the ground-based receiver [40]. At the present stage, a 64-pixel SSPD array with an area of $160 \times 160\,\mu m^2$ has been prepared and the signals from each pixel are merged by the custom SiGe cryogenic amplifier and combiner inside the cryocooler. It has been confirmed that the 63 pixels of 64 pixels have a single-photon counting ability and the combined SDE of 8 pixels reached 23% for free-space-coupled 1534-nm light. The maximum CR was also improved to 25 Mcps for 8 pixels compared to 3.4 Mcps for a single pixel. As a preliminary experiment, a real-time transmission involving a 1080p HDTV signal has been presented by using the developed 64-pixel SSPD array system. The TV signal was encoded to a pulse position modulation (PPM) serial signal and then converted to the optical signal by intensity modulation. The optical signal was coupled to the SSPD system in free space and decoded by a custom FPGA receiver. Toward the achievement of SSPD implementation in a 5-m-diameter telescope as a goal of the project, a 267-Mb/s PPM link is expected to be possible by operating the full 64-pixel SSPD array [40].

6. Life Science Applications

New trends in the application of SSPD to the life sciences field have also appeared. Gemmell *et al*. demonstrated singlet oxygen luminescence dosimetry (SOLD), which is crucial for ensuring optimal treatment in the clinical discipline, by using SSPD [48]. In many biological and physiological systems, the energy relaxation process of molecular oxygen from the excited singlet state (single oxygen) to the ground state is important. This process emits luminescence at a wavelength of approximately 1270 nm; thus, efficient near-infrared single-photon detection is essential to perform SOLD accurately. Conventionally, a specialized photomultiplier tube (PMT) with a low detection efficiency of less than 1% has been utilized and this limits the utility. Therefore, as shown in Fig. 2 (a), the authors applied an SSPD with an SDE of ~15% in fiber-based SOLD for the first time, and determined the signature of singlet oxygen luminescence by using a solution of Rose Bengal [48].

In the life science field, the use of weak light in the visible wavelength range is more common because the physical and chemical dynamics in biological samples can be obtained by detecting the fluorescence emitted by molecules. There are many useful methods that employ fluorescent photons, e.g., fluorescence recovery after photobleaching (FRAP), fluorescence loss in photobleaching (FLIP), fluorescence resonance energy transfer (FRET), and fluorescence correlation spectroscopy (FCS) [9]. In these experiments, it is crucial to ensure that the single-photon detector is capable of detecting the fluorescent photons efficiently. In Ref. [8], the authors optimized the optical design of the SSPD to enhance the absorptance at visible wavelengths by tuning the thickness of the dielectric cavity. Furthermore, in order to couple the incident light from large-core MM fiber efficiently, the size of the active area has been enlarged to form a 35-μm-diameter circle. As a result, a high SDE over 70% for visible wavelengths was achieved. As shown in Fig. 2 (b), a visible-wavelength SSPD was applied in an FCS experiment, which is a powerful tool for investigating the molecular motion of fluorescent materials in living cells as well as in aqueous solutions in vivo [9]. The FCS experiment measures the temporal autocorrelation of the flu-

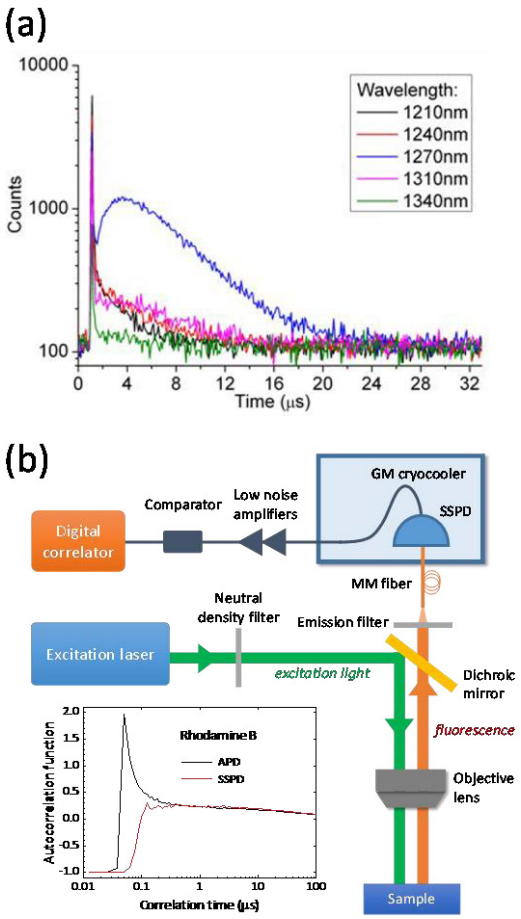

Fig. 2 (a) Representative TCSPC histograms from a Rose Bengal solution (250 μg/ml, 0.257 μM) with bandpass filters (20 nm spectral width) centered at 1210, 1240, 1270, 1310, and 1340 nm [48]. Short-lived fluorescence (occurring within the first μs) is present at all wavelengths studied; the key signature of $^1O_2$ is the onset and decay observed only at 1270 nm. (b) Schematics of the FCS system with SSPD [9]. Bottom left: Autocorrelation functions vs. correlation time of Rhodamine B. Black and red lines indicate data obtained by using APD and SSPD, respectively.

orescence emitted from the molecules in the observed region. The detection of fluorescent photons was conventionally performed by using Si APDs. Although Si APDs show a high detection efficiency of 60–70%, "afterpulsing," which is undesired pulse noise after photon detection, is a problem. Because this afterpulsing effect appears within several hundred nanoseconds, short-time-scale phenomena such as the rotational diffusion of molecules have not been observed in FCS measurements. On the other hand, SSPDs are free from afterpulsing; thus, they enable the measurement and analysis of the autocorrelation function in the sub-microsecond region (Fig. 2 (b), bottom left). The authors presented the clear advantage of the SSPD-FCS by using Rhodamine B and 6G as fluorescence specimens [9]. More recently, also for polarization-dependent FCS, it has been shown that the afterpulse-free SSPD has an advantage over Si APDs from the point of view of simple optical setup with good optical efficiency [10].

7. Quantum Optics and Other Applications

The characteristics of SSPDs also contribute significant benefits to quantum optics experiments. The characterization of single photon sources is an attractive application of SSPD. Hadfield *et al*. presented the coincidence (second-order correlation function, $g^{(2)}(\tau)$) measurement of 902-nm-wavelength photons emitted from an InGaAs quantum dot by using SSPD and Si APD [49]. The lower timing jitter of SSPD results in the non-zero delay peak $g^{(2)}(0)$ becoming narrower. The authors also presented the time-resolved measurement of the spontaneous emission lifetime of a quantum dot. They obtained a sharp rise in the histogram of the output because of the good timing resolution of the SSPD. Very recently, Miyazawa *et al*. demonstrated highly pure 1550-nm-wavelength single-photon emission from an InAs/InP quantum dot [50]. The authors fabricated the single-photon source with very low multiphoton emission probability and performed the $g^{(2)}(\tau)$ measurement by using high-performance SSPDs. As a result, they obtained a record value of 4.4×10^{-4} for $g^{(2)}(0)$ as shown in Fig. 3 (a), leading to a breakthrough toward the realization of a long-distance quantum communication system using single-photon sources [50].

Besides the characterization of a single-photon sources, practical SSPD systems with high SDE, low DCR, and excellent timing jitter have already been utilized for many quantum optics experiments such as entangled photon source demonstration and Hong-Ou-Mandel (HOM) interference experiments [51]. As a most recent example, Kobayashi *et al*. demonstrated HOM interference between two photons with wavelengths of different colors at 780 and 1522 nm, i.e., frequency-domain HOM interference [52]. In this experiment, SSPDs with a 60% SDE have been used and almost unity visibility of 0.98 was obtained indicating that the performance of the frequency-domain HOM interferometer was close to ideal.

Owing to their excellent timing resolution, the SSPDs can be utilized for fiber-dispersed Raman spectroscopy (FDRS) [53]. FDRS uses the difference in the time required for light of different wavelengths to travel through an optical fiber to obtain spectra by measuring the wavelength-dependent arrival time with a time-correlated single-photon counting module (TCSPC). Because the differences in the arrival time are extremely small, e.g., only 0.1 ns for a 1-nm wavelength difference (at a mean wavelength of 629 nm) even using a 200-m optical fiber, a detector with high timing resolution is essential. As shown in Fig. 3 (b), the authors demonstrated the basic concept of FDRS by using an SSPD with timing jitter of approximately 20 ps, and achieved a wavelength resolution of 3.42 nm at 629 nm [53].

The feature of high timing accuracy in SSPD has also contributed to the advance of time-of-flight (ToF) depth imaging (Fig. 3 (c)) [54]. The ToF technique enables the extraction of the distance to a target object by measuring the delay of reflected light pulses that are used to illumi-

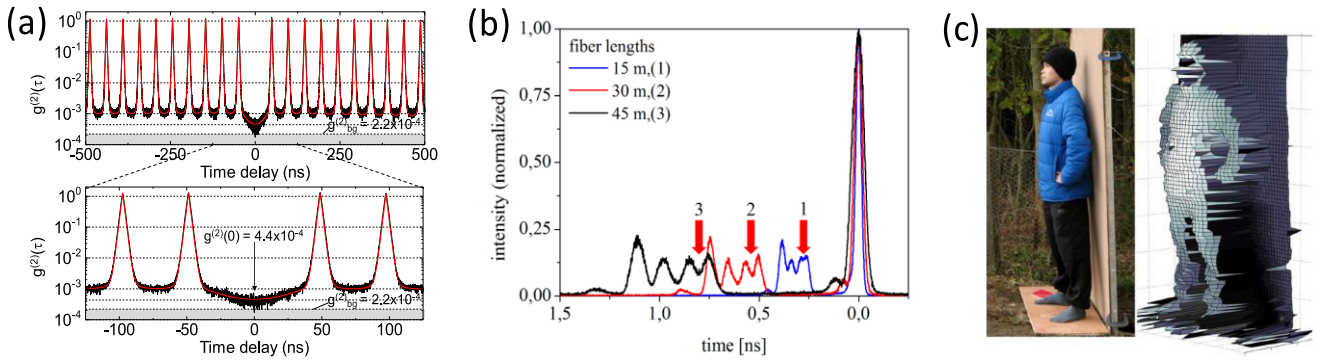

Fig. 3 (a) Calibrated $g^{(2)}(\tau)$ of the photo-emission from the exciton state shown on a semi logarithmic plot and enlarged plot of calibrated $g^{(2)}(\tau)$ around $\tau = 0$. The fit to the decay curve (red) demonstrates $g^{(2)}(0) = (4.4 \pm 0.2) \times 10^{-4}$ [50]. (b) Comparison of measurements with different fiber lengths with cyclohexane as sample, black = 15 m, red = 30 m, blue = 45 m [53]. Red arrows show the area where the improvement of the resolution by the use of a longer fiber can be seen. The separation of the two Raman bands is more clearly resolved for the 30-m long fiber. Further lengthening to 45 m does not improve the resolution any further and leads not only to a signal stretch but also to broadening of the Raman bands. (c) Depth profile measurements of humans, acquired in daylight at a standoff distance of 910 m [54].

nate the scene. Contrary to conventional ToF measurements that were made at wavelengths below 1000 nm, the adoption of SSPDs makes it possible to realize ToF imaging at 1560 nm, which has various advantages such as lower atmospheric attenuation, reduced solar background noise, and possible higher laser output power with eye safe.

For various applications such as spectroscopy, light source characterization, and photon statics, efficient single-photon detection in the middle-infrared wavelength region is also attractive. As described in Sect. 3, SSPDs intrinsically have a broadband sensitivity, and detection efficiency up to wavelengths of several micrometers has been reported [55]. In Ref. [55], the authors fabricated an ultra-narrow 30-, 50-, and 85-nm-wide NbN SSPD and measured the detection efficiency for the range 0.5–5 μm by using a broadband incoherent light source with a monochromator. They obtained a good detection efficiency of ~2% even at the longest wavelength of 5 μm for the 30-nm-wide SSPD. Although further improvement is still required for use in a practical system, the high potential of this SSPD as a promising candidate for a middle-infrared single-photon detector, which is still *missing*, has been shown.

Another interesting application of SSPD is for X-ray single-photon detection. Inderbitzin *et al.* fabricated a 100-nm-thick Nb meandering nanowire with a large active area of $131 \times 55\,\mu m^2$, and investigated its response to irradiation by X-ray sources [56]. As a result, continuous photon detection has been confirmed in the large spectral range of keV energies. Furthermore, the DCR of the SSPD is completely free for more than 5 hours even at a high bias current very close to the switching current.

Single-photon imaging by multi-pixel SSPD array also has been studied. As described in Sect. 3, 64-pixel SSPD arrays has already been developed, and their basic imaging function has been demonstrated [37], [38]. A key technique to realize the multi-pixel SSPD imaging system will be an efficient multiplex readout with fewer coaxial cables because the large number of the cables induce a head load into the cryocooler and thus the SSPD could not work [38], [39]. As another attractive way to realize an imaging function by SSPD, a compressive imaging with a single SSPD has been presented [57].

8. Conclusion

In this review, we introduced the photon detection mechanism and the current status of SSPD performance for various target wavelengths, and reviewed a wide range of SSPD applications including quantum communication, optical space telecommunication, and the life sciences. As described above, as a consequence of an enormous amount of effort, the overall performance of SSPD has already reached a practical level, and actually useful SSPD systems with a compact cryocooler have been realized and utilized in many areas of applied research. As the next step in the development of these systems, the improvement of the maximum counting rate is an important issue. The multi-element array structure is a key technology leading to the realization of ultrahigh-speed SSPD, and its readout and signal processing cryogenic technology need to be developed simultaneously. Different device structures such as the superconducting nanowire avalanche photodetector (SNAP) are also feasible for realizing a high counting rate and SDE in parallel [58]. In addition, the development of a highly efficient SSPD for longer wavelength photons such as those in the middle-infrared region is expected to have a huge impact on various research fields.

Acknowledgments

The authors thank M. Sasaki, M. Fujiwara, T. Haraguchi, Y. Hiraoka, M. Kinjo, J. Yamamoto, T. Yamamoto, N. Imoto,

Y. Nambu, T. Miyazawa, K. Takemoto, Y. Arakawa, and Z. Wang for fruitful discussion.

References

[1] G.N. Gol'tsman, O. Okunev, G. Chulkova, A. Lipatov, A. Semenov, K. Smirnov, B. Voronov, A. Dzardanov, C. Williams, and R. Sobolewski, "Picosecond superconducting single-photon optical detector," Appl. Phys. Lett., vol.79, no.6, pp.705, 2001.

[2] E.A. Dauler, M.E. Grein, A.J. Kerman, F. Marsili, S. Miki, S.W. Nam, M.D. Shaw, H. Terai, V.B. Verma, and T. Yamashita, "Review of superconducting nanowire single-photon detector system design options and demonstrated performance," Opt. Eng., vol.53, no.8, pp.081907-1-13, 2014.

[3] V. Anant, A.J. Kerman, E.A. Dauler, J.K.W. Yang, K.M. Rosfjord, and K.K. Berggren, "Optical properties of superconducting nanowire single-photon detectors," Opt. Exp., vol.16, no.14, pp.10750–10761, 2008.

[4] F. Marsili, V.B. Verma, J.A. Stern, S. Harrington, A.E. Lita, T. Gerrits, I. Vayshenker, B. Baek, M.D. Shaw, R.P. Mirin, and S.W. Nam, "Detecting single infrared photons with 93% system efficiency," Nat. Photon. vol.7, no.3, pp.210–214, 2013.

[5] D. Rosenberg, A.J. Kerman, R.J. Molnar, and E.A. Dauler, "High-speed and high-efficiency superconducting nanowire single photon detector array," Opt. Exp., vol.21, no.2, pp.1440–1447, 2013.

[6] S. Miki, T. Yamashita, H. Terai, and Z. Wang, "High performance fiber-coupled NbTiN superconducting nanowire single photon detectors with Gifford-McMahon cryocooler," Opt. Exp., vol.21, no.8, pp.10208–10214, 2013.

[7] A.R. Dixon, Z.L. Yuan, J.F. Dynes, A.W. Sharpe, and A.J. Shields, "Gigahertz decoy quantum key distribution with 1 Mbit/s secure key rate," Opt. Exp., vol.16, no.23, pp.18790–18797, 2008.

[8] D. Liu, S. Miki, T. Yamashita, L. You, Z. Wang, and H. Terai, "Multimode fiber-coupled superconducting nanowire single-photon detector with 70% system efficiency at visible wavelength," Opt. Exp., vol.22, no.18, pp.21167–21174, 2014.

[9] T. Yamashita, D. Liu, S. Miki, J. Yamamoto, T. Haraguchi, M. Kinjo, Y. Hiraoka, Z. Wang, and H. Terai, "Fluorescence correlation spectroscopy with visible-wavelength superconducting nanowire single-photon detector," Opt. Exp., vol.22, no.23, pp.28783–28789, 2014.

[10] J. Yamamoto, M. Oura, T. Yamashita, S. Miki, T. Jin, T. Haraguchi, Y. Hiraoka, H. Terai, and M. Kinjo, "Rotational diffusion measurements using polarization-dependent fluorescence correlation spectroscopy based on superconducting nanowire single-photon detector," Opt. Exp., vol.23, no.25, pp.32633–32642, 2015.

[11] A.D. Semenov, G.N. Gol'tsman, and A.A. Korneev, "Quantum detection by current carrying superconducting film," Physica C, vol.351, no.4, pp.349–356, 2001.

[12] L.N. Bulaevskii, M.J. Graf, and V.G. Kogan, "Vortex-assisted photon counts and their magnetic field dependence in single-photon superconducting detectors," Phys. Rev. B, vol.85, no.1, pp.014505-1-10, 2012.

[13] A.M. Kadin, M. Leung, and A.D. Smith, "Photon-assisted vortex depairing in two-dimensional superconductors," Phys. Rev. Lett., vol.65, no.25, pp.3193–3196, 1990.

[14] J.J. Renema, G. Frucci, Z. Zhou, F. Mattioli, A. Gaggero, R. Leoni, M.J.A. de Dood, A. Fiore, and M.P. van Exter, "Universal response curve for nanowire superconducting single-photon detectors," Phys. Rev. B, vol.87, no.17, pp.174526, 2013.

[15] J.J. Renema, R. Gaudio, Q. Wang, Z. Zhou, A. Gaggero, F. Mattioli, R. Leoni, D. Sahin, M.J.A. de Dood, A. Fiore, and M.P. van Exter, "Experimental Test of Theories of the Detection Mechanism in a Nanowire Superconducting Single Photon Detector," Phys. Rev. Lett., vol.112, no.11, pp.117604, 2014.

[16] A. Engel, A. Schilling, K. Il'in, and M. Siegel, "Dependence of count rate on magnetic field in superconducting thin-film TaN single-photon detectors," Phys. Rev. B, vol.86, no.14, pp.140506(R), 2012.

[17] Y. Ota, K. Kobayashi, M. Machida, T. Koyama, and F. Nori, "Full Numerical Simulations of Dynamical Response in Superconducting Single-Photon Detectors," IEEE Trans. Appl. Supercond., vol.23, no.3, pp.2201105–2201105, 2013.

[18] A.N. Zotova and D.Y. Vodolazov, "Photon detection by current-carrying superconducting film: A time-dependent Ginzburg-Landau approach," Phys. Rev. B, vol.85, no.2, pp.024509-1-9, 2012.

[19] H. Bartolf, A. Engel, A. Schilling, K. Il'in, M. Siegel, H.-W. Hübers, and A. Semenov, "Current-assisted thermally activated flux liberation in ultrathin nanopatterned NbN superconducting meander structures," Phys. Rev. B, vol.81, no.2, pp.024502-1-12, 2010.

[20] L.N. Bulaevskii, M.J. Graf, C.D. Batista, and V.G. Kogan, "Vortex-induced dissipation in narrow current-biased thin-film superconducting strips," Phys. Rev. B, vol.83, no.14, pp.144526, 2011.

[21] T. Yamashita, S. Miki, K. Makise, W. Qiu, H. Terai, M. Fujiwara, M. Sasaki, and Z. Wang, "Origin of intrinsic dark count in superconducting nanowire single-photon detectors," Appl. Phys. Lett., vol.99, no.16, pp.161105, 2011.

[22] T. Yamashita, S. Miki, H. Terai, and Z. Wang, "Low-filling-factor superconducting single photon detector with high system detection efficiency," Opt. Exp., vol.21, no.22, pp.27177–27184, 2013.

[23] V.B. Verma, B. Korzh, F. Bussières, R.D. Horansky, S.D. Dyer, A.E. Lita, I. Vayshenker, F. Marsili, M.D. Shaw, H. Zbinden, R.P. Mirin, and S.W. Nam, "High-efficiency superconducting nanowire single-photon detectors fabricated from MoSi thin-films," Opt. Exp., vol.23, no.26, pp.33792–33801, 2015.

[24] V.B. Verma, B. Korzh, F. Bussières, R.D. Horansky, A.E. Lita, F. Marsili, M.D. Shaw, H. Zbinden, R.P. Mirin, and S.W. Nam, "High-efficiency WSi superconducting nanowire single-photon detectors operating at 2.5 K," Appl. Phys. Lett., vol.105, no.12, pp.122601, 2014.

[25] V.B. Verma, A.E. Lita, M.R. Vissers, F. Marsili, D.P. Pappas, R.P. Mirin, and S.W. Nam, "Superconducting nanowire single photon detectors fabricated from an amorphous $Mo_{0.75}Ge_{0.25}$ thin film," Appl. Phys. Lett., vol.105, no.2, pp.022602, 2014.

[26] A.J. Miller, A.E. Lita, B. Calkins, I. Vayshenker, S.M. Gruber, and S.W. Nam, "Compact cryogenic self-aligning fiber-to-detector coupling with losses below one percent," Opt. Exp., vol.19, no.10, pp.9102–9110, 2011.

[27] S. Miki, T. Yamashita, M. Fujiwara, M. Sasaki, and Z. Wang, "Multi-channel SNSPD system with high detection efficiency at telecommunication wavelength," Opt. Lett., vol.35, no.13, pp.2133–2135, 2010.

[28] H. Shibata, K. Shimizu, H. Takesue, and Y. Tokura, "Ultimate low system dark-count rate for superconducting nanowire single-photon detector," Opt. Lett., vol.40, no.14, pp.3428–3431, 2015.

[29] K. Smirnov, Y. Vachtomin, A. Divochiy, A. Antipov, and G. Goltsman, "Dependence of dark count rates in superconducting single photon detectors on the filtering effect of standard single mode optical fibers," Appl. Phys. Exp., vol.8, no.2, pp.022501, 2015.

[30] T. Yamashita, S. Miki, W. Qiu, M. Fujiwara, M. Sasaki, and Z. Wang, "Temperature Dependent Performances of Superconducting Nanowire Single-Photon Detectors in an Ultralow-Temperature Region," Appl. Phys. Exp., vol.3, no.10, pp.102502, 2010.

[31] X. Yang, H. Li, W. Zhang, L. You, L. Zhang, X. Liu, Z. Wang, W. Peng, X. Xie, and M. Jiang, "Superconducting nanowire single photon detector with on-chip bandpass filter," Opt. Exp., vol.22, no.13, pp.16267–16272, 2014.

[32] T. Yamashita, K. Waki, S. Miki, R.A. Kirkwood, R.H. Hadfield, and H. Terai, "Superconducting nanowire single-photon detectors with non-periodic dielectric multilayers," Sci. Rep., vol.6, article number: 35240, 2016.

[33] W.J. Zhang, H. Li, L.X. You, J. Huang, Y.H. He, L. Zhang, X.Y. Liu, S.J. Chen, Z. Wang, and X.M. Xie, "Superconducting Nanowire Single-Photon Detector With a System Detection Efficiency Over 80%

at 940-nm Wavelength," IEEE Photon. J., vol.8, no.2, pp.4500908, 2016.
[34] H. Li, L. Zhang, L. You, X. Yang, W. Zhang, X. Liu, S. Chen, Z. Wang, and X. Xie, "Large-sensitive-area superconducting nanowire single-photon detector at 850 nm with high detection efficiency," Opt. Exp., vol.23, no.13, pp.17301–17308, 2015.
[35] H. Li, S. Chen, L. You, W. Meng, Z. Wu, Z. Zhang, K. Tang, L. Zhang, W. Zhang, X. Yang, X. Liu, Z. Wang, and X. Xie, "Superconducting nanowire single photon detector at 532 nm and demonstration in satellite laser ranging," Opt. Exp., vol.24, no.4, pp.3535–3542, 2016.
[36] A.J. Kerman, E.A. Dauler, W.E. Keicher, J.K.W. Yang, K.K. Berggren, G. Gol'tsman, and B. Voronov, "Kinetic-inductance-limited reset time of superconducting nanowire photon counters" Appl. Phys. Lett., vol.88, no.11, pp.111116, 2006.
[37] S. Miki, T. Yamashita, Z. Wang, and H. Terai, "A 64-pixel NbTiN superconducting nanowire single-photon detector array for spatially resolved photon detection," Opt. Exp., vol.22, no.7, pp.7811–7820, 2014.
[38] M.S. Allman, V.B. Verma, M. Stevens, T. Gerrits, R.D. Horansky, A.E. Lita, F. Marsili, A. Beyer, M.D. Shaw, D. Kumor, R. Mirin, and S.W. Nam, "A near-infrared 64-pixel superconducting nanowire single photon detector array with integrated multiplexed readout," Appl. Phys. Lett., vol.106, no.19, pp.192601, 2015.
[39] T. Yamashita, S. Miki, H. Terai, K. Makise, and Z. Wang, "Crosstalk-free operation of multielement superconducting nanowire single-photon detector array integrated with single-flux-quantum circuit in a 0.1 W Gifford-McMahon cryocooler," Opt. Lett., vol.37, no.14, pp.2982–2984, 2012.
[40] M.D. Shaw, F. Marsili, A.D. Beyer, J.A. Stern, G.V. Resta, P. Ravindran, S. Chang, J. Bardin, D.S. Russell, J.W. Gin, F.D. Patawaran, V.B. Verma, R.P. Mirin, S.W. Nam, and W.H. Farr, "Arrays of WSi Superconducting Nanowire Single Photon Detectors for Deep-Space Optical Communications," CLEO:2015, JTh2A.68.
[41] H.-K. Lo, M. Curty, and K. Tamaki, "Secure quantum key distribution," Nat. Photon., vol.8, no.8, pp.595–604, 2014.
[42] H. Takesue, S.W. Nam, Q. Zhang, R.H. Hadfield, T. Honjo, K. Tamaki, and Y. Yamamoto, "Quantum key distribution over a 40-dB channel loss using superconducting single-photon detectors," Nat. Photon., vol.1, no.6, pp.343–348, 2007.
[43] M. Sasaki, M. Fujiwara, H. Ishizuka, W. Klaus, K. Wakui, M. Takeoka, S. Miki, T. Yamashita, Z. Wang, A. Tanaka, K. Yoshino, Y. Nambu, S. Takahashi, A. Tajima, A. Tomita, T. Domeki, T. Hasegawa, Y. Sakai, H. Kobayashi, T. Asai, K. Shimizu, T. Tokura, T. Tsurumaru, M. Matsui, T. Honjo, K. Tamaki, H. Takesue, Y. Tokura, J.F. Dynes, A.R. Dixon, A.W. Sharpe, Z.L. Yuan, A.J. Shields, S. Uchikoga, M. Legré, S. Robyr, P. Trinkler, L. Monat, J.-B. Page, G. Ribordy, A. Poppe, A. Allacher, O. Maurhart, T. Länger, M. Peev, and A. Zeilinger, "Field test of quantum key distribution in the Tokyo QKD Network," Opt. Exp., vol.19, no.11, pp.10387–10409, 2011.
[44] H. Shibata, T. Honjo, and K. Shimizu, "Quantum key distribution over a 72 dB channel loss using ultralow dark count superconducting single-photon detectors," Opt. Lett., vol.39, no.17, pp.5078–5081, 2014.
[45] T. Inagaki, N. Matsuda, O. Tadanaga, M. Asobe, and H. Takesue, "Entanglement distribution over 300 km of fiber," Opt. Exp., vol.21, no.20, pp.23241–23249, 2013.
[46] Y.-L. Tang, H.-L. Yin, Q. Zhao, H. Liu, X.-X. Sun, M.-Q. Huang, W.-J. Zhang, S.-J. Chen, L. Zhang, L.-X. You, Z. Wang, Y. Liu, C.-Y. Lu, X. Jiang, X. Ma, Q. Zhang, T.-Y. Chen, and J.-W. Pan, "Measurement-Device-Independent Quantum Key Distribution over Untrustful Metropolitan Network," Phys. Rev. X, vol.6, no.1, pp.011024, 2016.
[47] M. Grein, E. Dauler, A. Kerman, M. Willis, B. Romkey, B. Robinson, D. Murphy, and D. Boroson, "A superconducting photon-counting receiver for optical communication from the Moon," SPIE, 2015.
[48] N.R. Gemmell, A. McCarthy, B. Liu, M.G. Tanner, S.D. Dorenbos, V. Zwiller, M.S. Patterson, G.S. Buller, B.C. Wilson, and R.H. Hadfield, "Singlet oxygen luminescence detection with a fiber-coupled superconducting nanowire single-photon detector," Opt. Exp., vol.21, no.4, pp.5005–5013, 2013.
[49] R.H. Hadfield, M.J. Stevens, S.S. Gruber, A.J. Miller, R.E. Schwall, R.P. Mirin, and S.W. Nam, "Single photon source characterization with a superconducting single photon detector," Opt. Exp., vol.13, no.26, pp.10846–10853, 2005.
[50] T. Miyazawa,, K. Takemoto, Y. Nambu, S. Miki, T. Yamashita, H. Terai, M. Fujiwara, M. Sasaki, Y. Sakuma, M. Takatsu, T. Yamamoto, and Y. Arakawa, "Single-photon emission at 1.5 μm from an InAs/InP quantum dot with highly suppressed multi-photon emission probabilities," Appl. Phys. Lett., vol.109, no.13, pp.132106, 2016.
[51] "Superconducting Devices in Quantum Optics," Eds. R.H. Hadfield and G. Johanson, Springer 2016.
[52] T. Kobayashi, R. Ikuta, S. Yasui, S. Miki, T. Yamashita, H. Terai, T. Yamamoto, M. Koashi, and N. Imoto, "Frequency-domain Hong–Ou–Mandel interference," Nat. Photon., vol.10, no.7, pp.441–444, 2016.
[53] J. Toussaint, S. Dochow, I. Latka, A. Lukic, T. May, H.-G. Meyer, K. Il'in, M. Siegel, and J. Popp, "Proof of concept of fiber dispersed Raman spectroscopy using superconducting nanowire single-photon detectors," Opt. Exp., vol.23, no.4, pp.5078–5090, 2015.
[54] A. McCarthy, N.J. Krichel, N.R. Gemmell, X. Ren, M.G. Tanner, S.N. Dorenbos, V. Zwiller, R.H. Hadfield, and G.S. Buller, "Kilometer-range, high resolution depth imaging via 1560 nm wavelength single-photon detection," Opt. Exp., vol.21, no.7, pp.8904–8915, 2013.
[55] F. Marsili, F. Bellei, F. Najafi, A.E. Dane, E.A. Dauler, R.J. Molnar, and K.K. Berggren, "Efficient Single Photon Detection from 500 nm to 5 μm Wavelength," Nano Lett., vol.12, no.9, pp.4799–4804, 2012.
[56] K. Inderbitzin, A. Engel, A. Schilling, K. Il'in, and M. Siegel, "An ultra-fast superconducting Nb nanowire single-photon detector for soft x-rays," Appl. Phys. Lett., vol.101, no.16, pp.162601, 2012.
[57] T. Gerrits, D. Lum, V. Verma, J. Howell, R. Mirin, and S.W. Nam, "Short-wave infrared compressive imaging of single photons," CLEO: Science and Innovations 2016, SM2E.4, 2016.
[58] M. Ejrnaes, R. Cristiano, O. Quaranta, S. Pagano, A. Gaggero, F. Mattioli, R. Leoni, B. Voronov, and G. Gol'tsman, "A cascade switching superconducting single photon detector," Appl. Phys. Lett., vol.91, no.26, pp.262509, 2007.

Taro Yamashita received his Ph.D. degree in physics from Tohoku University, Japan, in 2005. He is currently Senior Researcher at the Advanced ICT Research Institute, NICT, Japan. His research interests include superconducting devices and physics, single-photon detectors, and superconducting spintronics. He is a member of JSAP) and IEICE.

Shigehito Miki received his Ph.D. degree in electrical engineering from Kobe University, Japan, in 2002. He is currently Senior Researcher at the Advanced ICT Research Institute, NICT, Japan. His research interests include superconducting devices and physics, and single-photon detectors. He is a member of JSAP and IEICE.

Hirotaka Terai received the B.E., M.E. and Ph.D. degrees in electronics engineering in 1991, 1993, and 1996, respectively. During 1996–1997, he stayed in NEC Co. Ltd to study high-Tc superconducting devices and circuits. He currently is research manager at the Advanced ICT research institute in NICT, Japan. He is a member of IEICE and JSAP.